Applied Surface Science 428 (2018) 1070–1078

Contents lists available at ScienceDirect

Applied Surface Science

journal homepage: www.elsevier.com/locate/apsusc

Full Length Article

Structure and properties of polyaniline nanocomposite coatings containing gold nanoparticles formed by low-energy electron beam deposition

Surui Wang[a], A.A. Rogachev[a,b,*], M.A. Yarmolenko[a,c], A.V. Rogachev[a,b], Jiang Xiaohong[a], M.S. Gaur[d], P.A. Luchnikov[e], O.V. Galtseva[b], S.A. Chizhik[f]

[a] International Chinese-Belorussian Scientific Laboratory on Vacuum-Plasma Technology, College of Chemical Engineering, Nanjing University of Science and Technology, Nanjing 210094, China
[b] Tomsk Polytechnic University, 30, Lenin Avenue, Tomsk 634050, Russia
[c] Francisk Skorina Gomel State University, 104, Sovetskaya Street, Gomel 246019, Belarus
[d] Department of Physics, Hindustan College of Science and Technology, Farah, Mathura 281122, Uttar Pradesh, India
[e] Moscow Technological University (MIREA), 119454, Vernadsky 78, Moscow, Russia
[f] Laboratory of "Nano-Processes and Technologies", A.V. Luikov Heat and Mass Transfer Institute of the National Academy of Sciences of Belarus 15, P. Brovka Str., Minsk, 220072, Belarus

ARTICLE INFO

Article history:
Received 15 May 2017
Received in revised form
16 September 2017
Accepted 26 September 2017
Available online 28 September 2017

Keywords:
Electron beam deposition
Thin conductive polymer film
Polyaniline
Gold nanoparticles
Nanocomposite coating

ABSTRACT

Highly ordered conductive polyaniline (PANI) coatings containing gold nanoparticles were prepared by low-energy electron beam deposition method, with emeraldine base and chloroauric acid used as target materials. The molecular and chemical structure of the layers was studied by Fourier transform infrared, Raman, UV–vis and X-ray photoelectron spectroscopy. The morphology of the coatings was investigated by atomic force and transmission electron microscopy. Conductive properties were obtained by impedance spectroscopy method and scanning spreading resistance microscopy mode at the micro- and nanoscale.

It was found that the emeraldine base layers formed from the products of electron-beam dispersion have extended, non-conductive polymer chains with partially reduced structure, with the ratio of imine and amine groups equal to 0.54. In case of electron-beam dispersion of the emeraldine base and chloroauric acid, a protoemeraldine structure is formed with conductivity 0.1 S/cm. The doping of this structure was carried out due to hydrochloric acid vapor and gold nanoparticles formed by decomposition of chloroauric acid, which have a narrow size distribution, with the most probable diameter about 40 nm. These gold nanoparticles improve the conductivity of the thin layers of PANI + Au composite, promoting intra- and intermolecular charge transfer of the PANI macromolecules aligned along the coating surface both at direct and alternating voltage.

The proposed deposition method of highly oriented, conductive nanocomposite PANI-based coatings may be used in the direct formation of functional layers on conductive and non-conductive substrates.

1. Introduction

Polyaniline (PANI) and PANI-based nanocomposite coatings are the promising objects of research due to their functional properties that may be applied, such as efficient functional layers for the generation and storage of electric energy devices like solar cells and supercapacitors [1,2], for creation of biocompatible electromechanical devices, drug delivery systems [3], for environmental monitoring systems, for elaboration of highly sensitive and selective gas or ion-selective sensors [4,5], etc. The choice of polyaniline is caused by its high conductivity, chemical stability and the stability of its electrophysical properties, low cost of synthesis. The high functional properties of polyaniline are especially manifested in the micro- and nanostructured state, when the part of surface atoms increases significantly. In such systems, in addition to the chemical composition, the structural organization of polymer macromolecules and the distribution of the dopants have an impact [2,5–7]. It is well-known that PANI conductivity is due to the macromolecule portions protonated by acids [8], but for

* Corresponding author at: International Chinese-Belorussian Scientific Laboratory on Vacuum-Plasma Technology, College of Chemical Engineering, Nanjing University of Science and Technology, Nanjing 210094, China.

https://doi.org/10.1016/j.apsusc.2017.09.225
0169-4332/

disordered macromolecules of polymer, the conductivity remains low even for high degree of doping by acids [7,9,10].

Another promising way to increase the conductivity, sensing and catalytic properties of PANI layers is doping them with noble metal nanoparticles (Pd, Pt, Au), for which methods of electrochemical polymerization [11,12], including in-situ [13], solution preparation methods [4,14,15], self-assembly method [15], Langmuir-Blodgett [4] and etc., are applied.

The methods of electrochemical polymerization that combine the synthesis of PANI composite materials are widely applied [5,12,13]. However, the reactions underlying the method are complex, multistage, and they proceed simultaneously with the oxidative polymerization of aniline, which also complicates the control of the conditions for the preparation of composites. In addition, there remains the problem of transferring the formed layer from the electrodes to the working surface, using easily oxidized substrates [13]. This problem is solved by methods of self-organization from solutions for example Langmuir-Blodgett [4]. In this case, more ordered organization of the deposited molecules is possible due to the use of organophilic clay. However, the use of ligands to stabilize gold nanoparticles and the complex multicomponent dopants system slightly complicates the process of coating formation. The solution methods for the preparation of PANI-based coatings using various solvents have problems associated with their complete removal [14,16]. Besides, unsolved issues related to the molecular ordering of the formed layers remain [16]. The vacuum methods of PANI-based layer formation exist and are developing [1,17–20]. For example, by resistive evaporation of the initial polymer, it is possible to form an emeraldine coating [1], and its further doping is possible by dissolution methods [17], or vice versa, after the dissolution methods of PANI coatings synthesis, its may be doped by treating in oxygen plasma of high-frequency low-pressure discharge [18]. This approach makes it possible to use rigorously controlled and reproducible vacuum methods for obtaining thin films with a tailored structure and properties.

The main advantage of PANI-based coatings deposited by vacuum methods is the ability to form thin (less than a few micrometers) layers under rigorously controlled conditions onto conductive and non-conductive substrates, with the thickness specified. For a poorly soluble PANI it is a very important advantage, especially when using these coatings as sensor layers. A small thickness of the sample allows to increase the sensitivity and decrease the response time [4,5,15]. In addition, vacuum deposition methods make it possible to effectively solve the problem of adhesion to the substrate by physical pre-treatment (activation) procedures. However, the vacuum methods [17,18] of PANI conductive layers described are not completely solvent-free and require additional operations outside the vacuum.

We are developing a completely solvent-free plasma-chemical method for obtaining conductive composite PANI coatings from the products of electron-beam dispersion in the vacuum of emeraldine base and the corresponding dopant. This method has been implemented for one-step synthesis of non-conductive and conductive PANI-based coatings, including those containing silver nanoparticles [19,20]. The minimal effect of the PANI decomposition products on the substrate makes it possible to use conductive or non-conductive materials, including those having a low heat resistance. The objective of this paper is to study the possibility of forming thin PANI coatings containing gold nanoparticles and to investigate their structure and electrical properties.

2. Experimental

The PANI + Au coatings were deposited from the active gas phase generated by electron-beam dispersion (EBD) of a mechanical mixture of PANI (emeraldine base form with average molecular weight $M_w = 5000$, Aldrich) and chloroauric acid ($HAuCl_4 \cdot 4H_2O$, Aladdin) in a weight ration 1–2. The thickness of PANI-based coatings was controlled during the deposition using a quartz crystal microbalance (QCM) and it was equal to 100 nm. The substrates were quartz and sodium chloride (NaCl) plates for spectroscopic measurements, interdigital capacitor with aluminum electrodes for impedance spectroscopy and atomic-force microscopy study. A more detailed description of the deposition technique is given in [19,20].

The molecular structure of the deposited coatings was studied by infrared spectroscopy method with Fourier transform infrared (FTIR) spectrophotometer Vertex-70 (Bruker) using a standard transmission cell and the Senterra (Bruker) Raman spectrometer with 532 nm excitation laser and a power of up to 5 mW. The UV–vis spectroscopy studies were carried out using the Cary-50 (Varian) ultraviolet/visible spectrophotometer.

The chemical structure of the deposited coatings was studied by XPS methods using a PHI Quantera II (Ulvac-PHI, Inc.) spectrometer. The emission of photoelectrons occurred under X-ray radiation from a source with characteristic lines of AlKα (1486.7 eV). The C1s peak with 284.6 eV binding energy position was used to compensate the surface-charging effects.

The morphology of the coatings was determined by transmission electron microscopy (TEM) using the JEM 2100 (Jeol) electron microscope. The PANI + Au coatings were deposited directly onto the copper grid substrate. To study the surface morphology a scanning probe microscope Solver P47 PRO (NT-MDT) was used. The scanning was carried out simultaneously in the contact and the spreading resistance mode with a probe of the CSG01 series with a conducting gold coating. In this case, apart from the topography of the surface, data on local conductivity were obtained by measuring the current value between the sample and the probe, with applied voltage amplitude of 2 V.

The coating under study was also deposited onto a substrate, which is an interdigital capacitor with aluminum electrodes (220 nm height, 50 μm width and 20 μm of electrode period), and the volt-ampere and frequency dependences of the complex impedance Z were measured. The measurements were done with the E7-20 immittance meter (MNIPI), with a step change in frequency f from 25 Hz to 10^6 Hz with measuring signal amplitude of 1 V. The minimum frequency change step less than 1 kHz was 1 Hz, over 1 kHz – 1 kHz. At each frequency step, the impedance Z and the phase shift angle φ between the current and the voltage of the capacitor under study were measured. The values of the real Z' and imaginary Z" components of the resistance, conductivity, imaginary component of the electric modulus M" were calculated based on known expressions for the impedance spectroscopy [21].

3. Results and their discussion

3.1. FTIR and Raman spectroscopy study of deposited coatings

The FTIR spectra of the PANI-based coatings and initial PANI powder (Fig. 1) allow of establish their structural differences. Only the initial emeraldine base powder and the coatings based on it have an absorption band at 3390 cm^{-1}, which indicates the presence of free secondary amine groups (—NH—) in the structure [1]. The PANI + Au coatings lack it, but intense enough absorption bands at 3200–2600 cm^{-1} are observed, responsible for the vibrations of secondary amine and protonated imine groups (—NH^+=) [22]. In general, a wide absorption band at more than 2000 cm^{-1} is considered by several authors a characteristic of conductive forms of polyaniline [22,23]. For these systems, in addition to an intensive absorption in the frequency range of 3200...2600 cm^{-1}, an

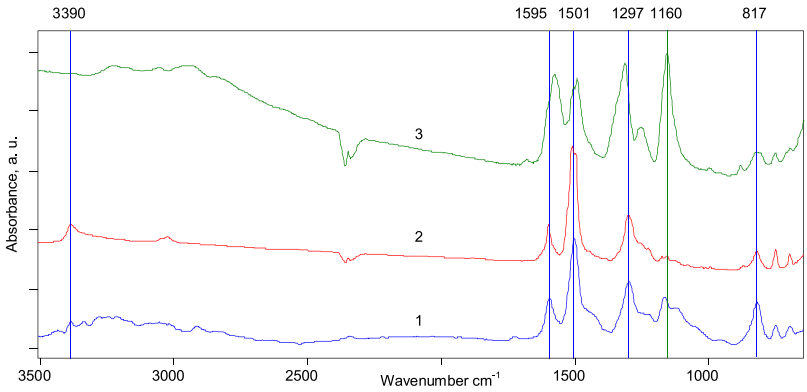

Fig. 1. FTIR spectra of initial PANI powder (1), coatings formed by EBD of PANI (2), PANI + Au (3).

absorption in the frequency range of 1100...1160 cm^{-1} is also observed, which characterized the degree of electrons delocalization, as well as indicates the presence of conducting regions in PANI-based coatings [8,11]. The intensity of the band at 1160 cm^{-1} is proportional to the degree of protonation of the PANI chains by acids [11]. The absorption band near 1300 cm^{-1}, responsible for the stretching vibrations of C—N groups of secondary aromatic amine, also increases with protonation [6], which is associated with an increase in the dipole moment of these vibrations in the presence of positive H^+ ions. A strong shoulder near 1340 cm^{-1}, absent from PANI coatings, may be associated with a specific interaction of gold atoms with the nitrogen atoms of the PANI main chain [11,12]. In addition to delocalization of electrons, in joint dispersion of the PANI and chloroauric acid mixture, structural transformations in the PANI main chain occur, which is indicated by a significant shift (up to 16 cm^{-1}) to the lower frequencies of quinonoid groups (Q) at 1595 cm^{-1} and benzene groups (B) bands, active at 1501 cm^{-1}. These shifts are possible in the composite PANI-based layers that contain ions or nanoparticles of transition metals in electrochemical synthesis. Moreover, these ions, depending on the electrode potential, are capable to attack quinonoid or benzene molecules, thus forming polaron structures in the polymer chain [14]. The significant impact of gold nanoparticles on the state of benzene and quinonoid rings is also evidenced by the substantial broadening of the absorption bands at 800–900 cm^{-1}, responsible for the deformation vibrations of the aromatic or quinonoid ring and the out-of-plane vibrations of the C—H groups [6].

In general, according to the FTIR spectroscopy data, we may note a large degree of polarons delocalization in thin-film systems formed by electron-beam dispersion of PANI + $HAuCl_4$ mixed targets, significant structural changes in the main chain, as well as a possible interaction of gold nanoparticles and their ions with aromatic and quinonoid rings of the macromolecule's main chain.

When studying the synthesized coatings using the Raman spectroscopy, it was taken into consideration that the intensity and position of the Raman spectra bands strongly depend on the wavelength of the exciting radiation. In addition, this radiation may initiate chemical and structural transformations in PANI, therefore, the studies were carried out with minimal power and time exposure to the sample. The analysis of the spectra obtained (Fig. 2) establishes that the initial PANI powder is characterized by three most intense absorption bands at 1584, 1474 and 1158 cm^{-1}, responsible for C—C stretching modes of benzene rings, stretching modes of C═N groups in quinonoid portions and bending modes of the C—H group in benzene and quinonoid rings, respectively [7,24]. After deposition, in PANI coatings the peak at 1474 cm^{-1} disappears, which indicates, first of all, the change in the conformation of the macromolecule from coiled to extended [7], and a peak near 1604 cm^{-1} appears, responsible for the stretching modes of C═C groups of the quinonoid fragment, and it is protonated to the reduced semi-quinonoid structure [25]. The obtained data correlate with previously published studies of vacuum layers using infrared spectroscopy, indicating the formation of a more reduced structure of PANI coatings, compared with the initial polymer [1,20].

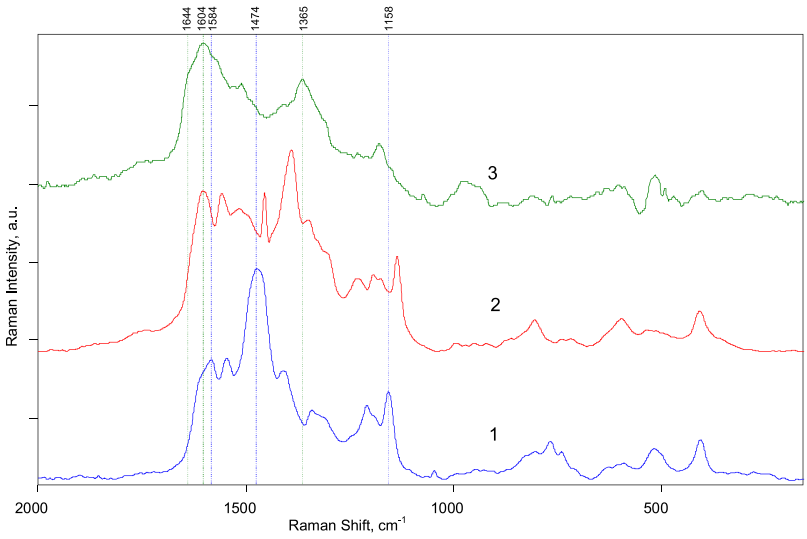

Fig. 2. Raman spectra of initial PANI powder (1), coatings formed by EBD of PANI (2), PANI + Au (3).

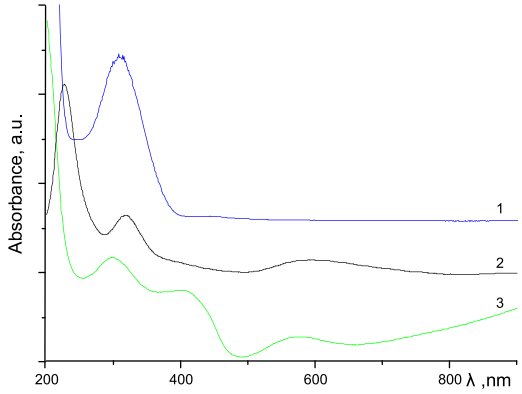

Fig. 3. UV–VIS absorbance spectra of coatings formed by EBD of PANI (1), $HAuCl_4$ (2), PANI + Au (3).

The Raman spectra of the coatings obtained by dispersing PANI and chloroauric acid confirm the FTIR spectroscopy data on a high degree of doping PANI-based coatings and the formation of a conducting structure (Fig. 2). This is evidenced by a broad peak near 1584 cm^{-1}, the simultaneous appearance of an intense peak at 1365 cm^{-1} that confirms the formation of delocalized polaron structures [26,27]. When a single-component PANI coating is deposited, the formation of delocalized polaron structures is not observed, but only the peak at 1474 cm^{-1} disappears. A shoulder near 1644 cm^{-1} established in PANI + Au coatings indicates the presence of tertiary amine groups, cross-linked structures [23,28]. However, the lack of a pronounced peak at 575 cm^{-1} in all the spectra of the coatings indicates significant differences in the formed structures from the previously considered cross-linked polymer network based on PANI [28].

The obtained results indicate the formation of flat, elongated, reduced chains after electron-beam dispersion of PANI, with the high value of their spread along the length. In the joint dispersion of emeraldine base and chloroauric acid, conductive (doped) PANI chains are formed, whose linear structure is high enough, with gold nanoparticles synthesized between the chains of macromolecules. These data can indicate the formation of flat ordered PANI layers and polyconjugate structures with facilitated interchain transfer of charge, which should increase the conductivity of the entire thin-film system.

3.2. UV–vis spectroscopy and TEM study of the formed coatings

In the UV–vis spectra of the coating (Fig. 3) deposited from emeraldine base, only one intense broad band with the maximum near 310 nm was established. This band may be considered a superposition of bands of the leucoemeraldine (not oxidized) PANI form with the maximum of less than 300 nm and the band at 325 nm due to π-π^* transitions in benzene rings of PANI [29]. A weak absorption band with the maximum near 450 nm is characteristic for localized polaron structures of protonated emeraldine [30]. The low optical density of the band at 625 nm, responsible for the exciton absorption of quinoid fragments, may indicate a reduced structure of PANI and a low molecular weight of the deposited layers [25,31].When $HAuCl_4$ and PANI are co-dispersed, the coatings spectra bands show the formation of radical cations (near 425 nm), polarons (near 780 nm), delocalized radical cations (>800 nm), which indicates the presence of conductive PANI states [32]. For the PANI + Au coating, a band of plasmon absorption of gold nanoparticles with the maximum at 570 nm was also established. This fact indicates the formation of gold nanoparticles of up to 100 nm diameter. The plasmon absorption peaks shifting may not only correlate with clusters size and shape, but also the dielectric constant of the polymer matrix [33].

Table 1
Results of N1s core-level spectra decomposition of initial PANI and PANI-based coatings.

Samples	Relative area of the N1 s components according to XPS data			
Group	—N=	—NH—	N^+	—N=/—NH—
Binding Energy, eV	398.5	399.6	400	–
Initial PANI	0.45	0.51	0.04	0.88
PANI coating	0.35	0.65	0	0.54
PANI + Au coating	0.18	0.74	0.08	0.24

In the coatings formed by EBD of $HAuCl_4$, in UV–vis spectrum, two intense peaks near 230, 320 nm and a broad peak with the maximum near 580 nm are observed. The peaks with the maxima at 230 and 320 nm are due to the absorption of $AuCl_4^-$ ions [12], and near 580 nm due to the absorption in the presence of gold nanoparticles [33,34]. The red shift of this absorption maximum, its lower intensity and greater width compared with the peak of the PANI + Au coating may indicate a broader size distribution of the formed gold nanoparticles [33,35]. The obtained results are confirmed by the TEM data presented in Fig. 4, according to which, PANI + Au coating has narrower size distribution of gold nanoparticles compared with $HAuCl_4$. It should be noted that both size distributions are not monodisperse, which indicates the complex, multistage route formation of the gold nanoparticles observed.

3.3. The XPS study of the deposited PANI-based coatings

The elemental analysis of the chemical structure using XPS methods allowed determining the features of the chemical state of the elements in the synthesized coatings.

In the XPS spectra of PANI + Au coatings, the presence of metallic gold Au^0 was established, as evidenced by the doublet of the emission peak at 84.4 eV ($4f_{7/2}$) and 88.1 eV ($4f_{5/2}$) (Fig. 5a). The lack of Au^{3+} ions with a doublet peak near 90 eV ($4f_{5/2}$) and 87 eV ($4f_{7/2}$) is confirmed by the lack of the Au^{3+} ($4f_{5/2}$) peak in XPS spectrum [5]. The obtained results are in complete agreement with the data of visible spectroscopy, according to which the presence of $AuCl_4^-$ anions in the formed layers is not established.

To evaluate the impact of the electron beam on the deposition processes and to analyze the obtained data, studies of the coating formed from the products of electron-beam dispersion of only $HAuCl_4$ were carried out. According to the XPS data, a more complex spectrum of Au 4f emission peaks is established. Its profile indicates the presence, apart from metallic atoms of Au^0, of also Au^{3+}, e.g., due to the presence of $AuCl_4^-$ anions, which is confirmed by the decomposition of the XPS spectrum into two pairs of peaks 84.1/87.1 and 86.5/90.2 (Fig. 5b) [12]. In this connection, one may assert about primary reconstruction of gold nanoparticles from $HAuCl_4$ in the joint electron-beam dispersion of PANI and $HAuCl_4$ and the key role of PANI in this process.

The XPS method allows determining the degree of oxidation and protonation of the PANI chains, by analyzing the N1 s peaking in this case (Fig. 6). It is known that the observed broad nitrogen peak may be decomposed into imine —N=, amine —NH— components, and positively charged N^+ ions with 398.5, 399.6 and more than 400 eV binding energies, respectively [2,36].

The quantitative analysis of the core-level N1 s peak components of the initial PANI powder, PANI and PANI + Au coatings using EBD (Fig. 6a – c) establishes significant differences in their chemical structure, as presented in Table 1.

It was found that in the EBD process, the degree of oxidation of the PANI coating (areas ratio —N=/—NH—), compared with the ini-

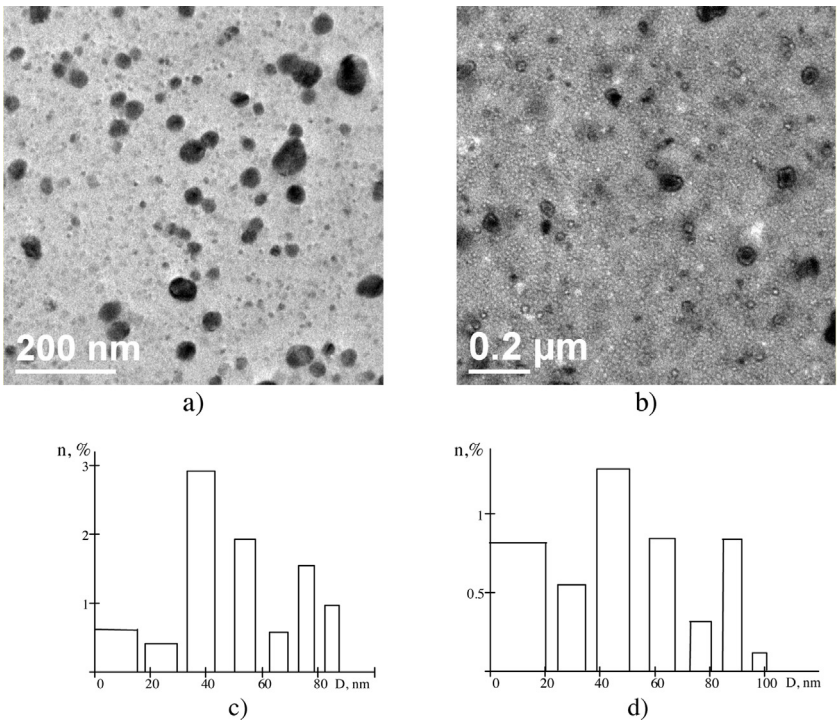

Fig. 4. TEM image and gold nanoparticles size distribution in PANI + Au (a, c) and $HAuCl_4$ (b, d) coatings.

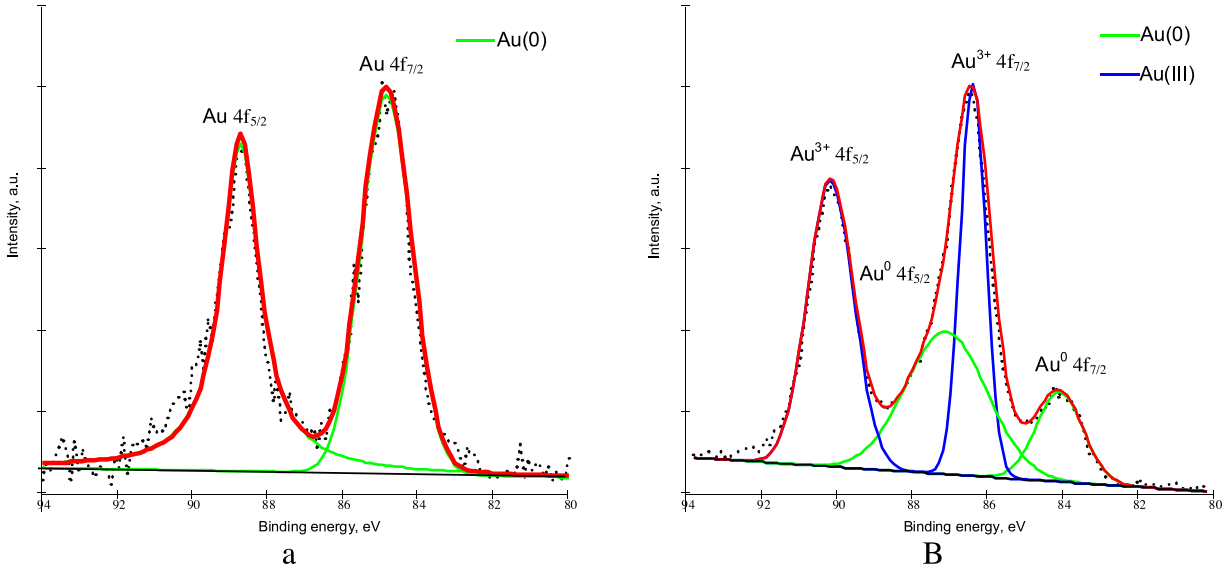

Fig. 5. Au4f XPS core-level spectra of PANI + Au (a) and $HAuCl_4$ (b) coatings.

tial polymer, decreases by more than 1.6 times, with more than 3.6 times when the composite target of PANI and $HAuCl_4$ is dispersed, and corresponds to the chemical structure of protoemeraldine [37]. This fact indicates active reduction processes under EBD, when a non-self-sustained plasma discharge burns in dispersed products. Moreover, not only PANI fragments, but also the gold nanoparticles formed from the $HAuCl_4$ dispersion products are reduced. It might be noted that the most probable is the reduction process of gold in the crucible, where the gold clusters form and are then transferred to the substrate surface and participate in coating growth.

The protonation of PANI chains is possible by the interaction of the formed hydrochloric acid vapor during the decomposition of $HAuCl_4$, which, according to the work [34], can already proceed at sufficiently low temperatures up to 110 °C. The protonation of PANI by the vapor of the formed acid is also confirmed by XPS data (Fig. 6d) in the analysis of high-resolution Cl2p peaks, which indicate the presence of two expressed Cl2p peaks at 197.1 eV and 198.6 eV, responsible for the anion of chlorine and the anion bounded with the positive radical of PANI, respectively [37,38]. The probability of this process is negligible, as evidenced by the low intensity of the Cl2p peaks, as well as the N^+ peak. The degree of protonation of PANI + Au coating increases twice as compared to the initial PANI powder, but it remains low enough and is less than 10% of the total number of nitrogen atoms, which cannot explain the high density of free radicals determined by FTIR, Raman and UV–vis spectroscopy methods. Apparently, the synthesized gold nanoparticles also participate in the formation of conductive chain fragments, which, on the one hand, reduce the degree of cross-

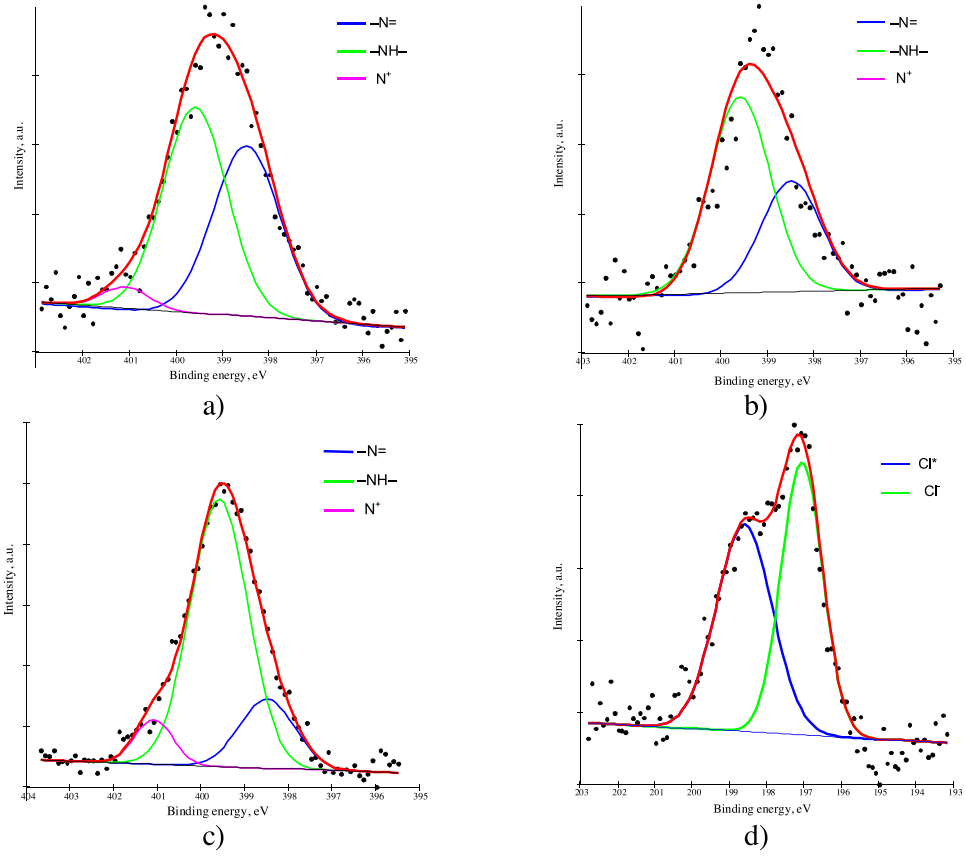

Fig. 6. XPS deconvoluted core-level spectra N1s of initial PANI (a), PANI coating (b) and PANI + Au coating (c), Cl2p (d) of PANI + Au coating.

linking of PANI macromolecules, and on the other hand, interacting with amine and imine groups, they contribute to an increase in the conductivity of the PANI-based coatings.

3.4. Electrophysical properties of PANI + Au coatings

The electrophysical properties of PANI-based coatings were studied by impedance spectroscopy and by plotting current-voltage characteristics. It was found that a typical current-voltage characteristic of the PANI + Au coating has a form of a curve with an initial non-linear region up to 1.4 V and virtually linear ohmic dependence at high voltages (Fig. 7). This type of dependence indicates the heterogeneity of the coating, where features of both semiconductor and metallic conductivity may manifest themselves.

A detailed analysis of such complex systems may be done by impedance spectroscopy method. Investigating the impedance spectra at different bias voltages (U_{bias}) in the range up to 2 V, the graphs of the frequency dependences of the real and the imaginary parts values of the resistance (Z', Z"), the imaginary part of the electric modulus (M") and Nyquist plot were plotted.

The frequency dependences of the real and imaginary part of resistance (Z', Z") of the PANI + Au coating (Fig. 8a, b) at the frequencies up to 10 kHz strongly depend on the U_{bias} value and are virtually independent on it at high values of the applied voltage frequency.

Moreover, as the applied bias voltage increases, the active and reactive resistance of the system at these frequencies decreases. Since the coatings were formed onto an interdigital capacitor with aluminum electrodes, according, e.g., [39], it may be asserted that it is the thin interfacial layer of the coating – the aluminum electrode – that makes the main contribution to the observed features of the

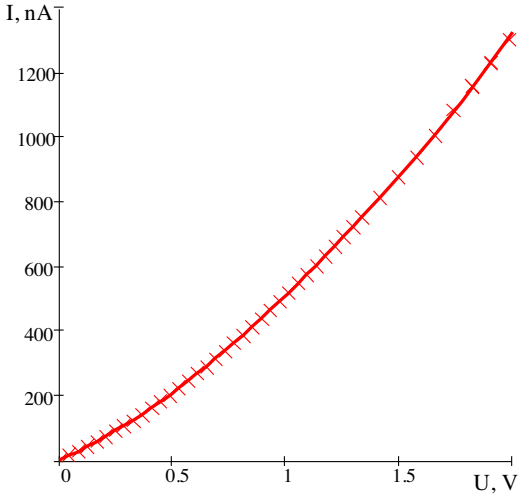

Fig. 7. I versus U measurements of PANI + Au coating.

I(U) graphs at low applied voltages and low frequencies (f < 10 kHz) of the dependences Z'(f) and Z"(f). The calculation of the conductivity real part, according to the known expression $Z'/((Z')^2 + (Z")^2)$ and 90 nm thickness, shows that at frequencies up to 10^4 this value is 0.1 S/cm, which exceeds the known values of the conductivity of PANI films by 1 or 2 orders, with a degree of doping by acids of about 10% [37].

The features of the electrophysical properties of the PANI + $HAuCl_4$ deposited coatings will be considered based on the analysis of the high-frequency part of the established

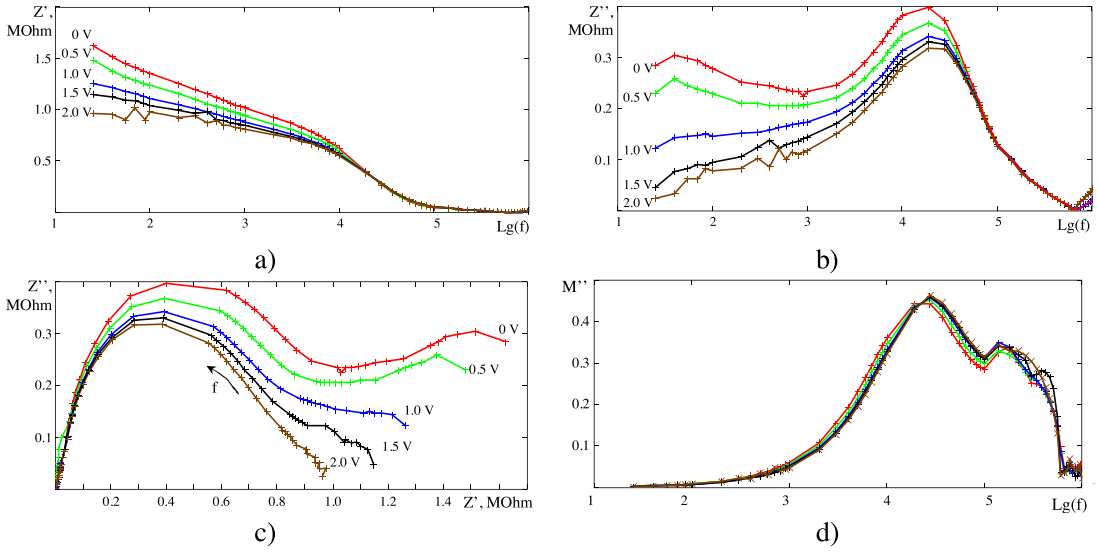

Fig. 8. Impedance spectra of PANI + Au coating, real Z' (a), imaginary Z" (b) part of impedance against frequency and Nyquist plot (c), imaginary part of electric module M" against frequency (d) at various bias potentials (U_{bias} = 0, 0.5, 1, 1.5, 2 V).

Nyquist plot and frequency dependences of the electric modulus M" imaginary part (f) (Fig. 8c, d).

The high-frequency part of the hodograph (Fig. 8c) has the form of a semicircle whose center is shifted downward relative to the horizontal axis. According to the known notions, such circles correspond to an equivalent replacement circuit that consists of a whole set of parallel impedances and capacitances of various denominations modeling a set of dipoles with different relaxation time constant τ_n, for the description of which the concept of CPE (constant phase element) is used [21]. The total resistance of this element can be described as $Z = R/(1 + (i\omega\tau)^s)$, where τ is the effective time constant that characterizes the distribution maximum τ_n and s is the parameter characterizing the displacement of the semicircle center relative to the Z' axis, which is responsible for the distribution width of relaxing elements. To analyze the relaxation time data, it is possible to use the dependences that consider only the dielectric polarization of the set of dipoles in question, such as the frequency dependence of the imaginary part of the electric modulus M" (Fig. 8d). This dependence is a curve that has at least 3 maxima in the high-frequency region, which, U_{bias} increas-

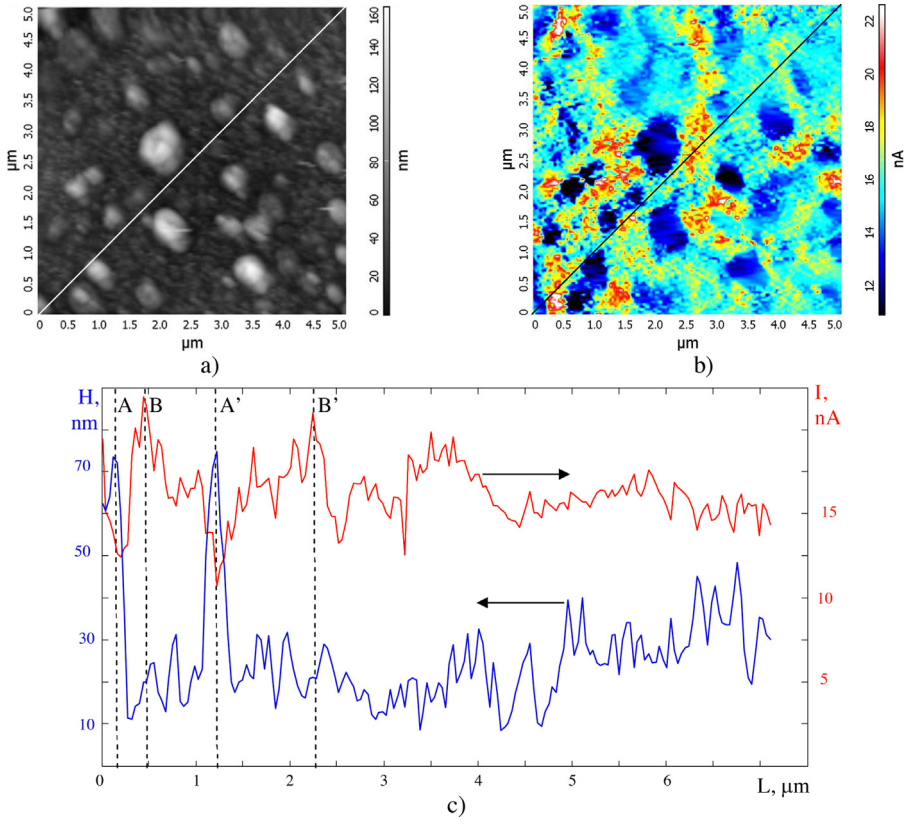

Fig. 9. Topography and spreading resistance mode data of atomic-force microscopy of PANI + Au coating.

ing slightly shift to higher frequencies. Each of these maxima can be characterized by the effective relaxation time constant equal to $1/f_{max}$, which will determine the individual relaxing element of our coatings. According to the previously obtained data and the papers by other authors [9,20], oxidized (imine) and reduced (amine) group of the PANI polymer chain may be chosen as such elements. In these studies we have established a more complex structure of the spectrum M"(f), which indicates the formation of additional relaxation chain portions formed, e.g., by a specific non-covalent interaction of PANI and gold nanoparticles.

The data of local electrophysical properties by the spreading resistance method indicate that the formed layers have a high inhomogeneity of conductivity at the micro- and nanoscale (Fig. 9a, b).

In particular, the low conductivity of large structural formations (grains) with a diameter of up to 500 nm and a height of up to 80 nm that constitute the coating has been established. Higher conductivity, as a rule, was observed in smoother structural formations. This conclusion is confirmed by a comparative analysis of surface profiles and the distribution of current values (Fig. 9c), according to which the minima of current values on the surface profile correspond to the largest minima on the surface profile (Fig. 9b, sections A, A'). These formations are most likely formed as a result of the droplet formation mechanism of the coating under electron-beam dispersion of the initial polymer [20]. One may also note the presence of slightly smaller grains up to 30 nm in height (Fig. 9c, sections B, B') that, on the contrary, have maximum conductivity. These structural formations apparently match the gold nanoclusters covered with a layer of PANI. Smoother portions of the coating correspond to the layer of PANI formed as a result of absorption processes and the polymerization of low-molecular fragments – the products of electron-beam dispersion of the initial PANI. These processes occur in the field of action of the substrate forces; besides, the off-oriented molecules have a greater probability of desorption. This facilitates the formation of the PANI layers predominantly aligned in the plane of the substrate, which is also confirmed by Raman spectroscopy.

4. Conclusion

The deposition of highly ordered thin layers of emeraldine base by electron-beam dispersion is established. When the target is exposed by the electron beam, volatile PANI fragments are formed, which, being absorbed on the substrate, polymerize again, thus forming loosely bounded PANI chains oriented mainly along the substrate surface. In addition, these fragments are reduced, the concentration of quinoid groups significantly decreases according to the data of FTIR, Raman and X-ray spectroscopy.

When used a mixture of emeraldine base and chloroauric acid such as target, intensive processes of decomposition of chloroauric acid occur, with gold clusters and hydrochloric acid vapor formed, which actively participate in the formation of conductive PANI coatings. These processes occur mainly in the target. Hydrochloric acid vapor dopes the PANI chains growing on the substrate, thus forming conductive areas, which is confirmed by FTIR, Raman, X-ray and impedance spectroscopy data. However, the concentration of such conductive regions is not large, and gold clusters keep the main contribution to the formation of the conductive PANI structure. They form gold nanoparticles, which influence also on the main orientation of PANI macromolecules along the substrate surface, embedded between growing chains. These particles have a narrow size distribution with the most probable diameter about 40 nm. They improve the conductivity of the thin-layer PANI + Au composite, promote intra- and intermolecular charge transfer of the PANI macromolecules aligned along the substrate surface at direct and alternating voltage.

The proposed method of highly oriented conductive PANI-based coatings deposition may be used for functional layers formation on substrates of various types and purposes.

References

[1] Mihai Irimia-Vladu, Nenad Marjanovic, Angela Vlad, Alberto Montaigne Ramil, Gerardo Hernandez-Sosa, Reinhard Schwodiauer, Siegfried Bauer, Niyazi Serdar Sariciftci, Vacuum-processed polyaniline-C 60 organic field effect transistors, Adv. Mater. 20 (2008) 3887–3892.

[2] Zhongqiu Tong, Yongning Yang, Jiayu Wang, Jiupeng Zhao, Bao-Lian Su, Yao Li, Layered polyaniline/graphene film from sandwich-structured polyaniline/graphene/polyaniline nanosheets for high-performance pseudosupercapacitors, J. Mater. Chem. A 2 (2014) 4642–4651.

[3] Luiz M. Lira, Susana I. Cordoba de Torresi, Conducting polymer-hydrogel composites for electrochemical release devices: synthesis and characterization of semi-interpenetrating polyaniline-polyacrylamide networks, Electrochem. Commun. 7 (2005) 717–723.

[4] A. De Barros, J.L. Constantino, J.R.R. Bortoleto, N.C. Da Cruz, M. Ferreira, Incorporation of gold nanoparticles into Langmuir-Blodgett films of polyaniline and montmorillonite for enhanced detection of metallic ions, Sens. Actuators B 236 (2016) 408–417.

[5] Sunil Dutt, Prem Felix Siril, Vipul Sharma, Selvakannan Periasamy, Gold core – polyaniline shell composite nanowires as substrate for surface enhanced Raman scattering and catalyst for dye reduction, New J. Chem. 39 (2015) 902–909.

[6] Miroslava Trchov, Jaroslav Stejskal, Polyaniline: the infrared spectroscopy of conducting polymer nanotubes (IUPAC technical report), Pure Appl. Chem. 83 (2011) 1803–1817.

[7] Qin Yao, Qun Wang, Liming Wang, Lidong Chen, Abnormally enhanced thermoelectric transport properties of SWNT/PANI hybrid films by the strengthened PANI molecular ordering, Energy Environ. Sci. 7 (2014) 3801–3807.

[8] Ivana Sedenkov, Miroslava Trchov, Jiri Dybal, Jaroslav Stejskal, Interaction of polyaniline film with dibutyl phosphonate versus phosphite: enhanced thermal stability, Polym. Degrad. Stab. 134 (2016) 357–365.

[9] B.G. Soares, Maria Elena Leyva, Guilherme M.O. Barra, Dipak Khastgir, Dielectric behavior of polyaniline synthesized by different techniques, Eur. Polym. J. 42 (2006) 676–686.

[10] Jiansheng Wua, Yimeng Sunb, Wei Xub, Qichun Zhanga, Investigating thermoelectric properties of doped polyaniline nanowires, Synth. Met. 189 (2014) 177–182.

[11] M. Hasik, C. Paluszkiewicz, E. Wenda, Interaction between polyanilines and platinum(IV) ions: vibrational spectroscopic studies, Vibr. Spectr. 29 (2002) 191–195.

[12] John M. Kinyanjui, David W. Hatchett, J. Anthony Smith, Mira Josowicz, Chemical synthesis of a polyaniline/gold composite using tetrachloroaurate, Chem. Mater. 16 (2004) 3390–3398.

[13] M.A. Shishov, V.A. Moshnikov, Sapurina I. Yu, Deposition of polyaniline layers with controlled thickness and morphology by in situ polymerization, Russ. J. Appl. Chem. 86 (2013) 51–62.

[14] O.P. Dimitriev, Doping of polyaniline by transition-metal salts, Macromolecules 37 (2004) 3388–3395.

[15] Chunhua Liu, Huiling Tai, Peng Zhang, Zongbiao Ye, Yuanjie Su, Yadong Jiang, Enhanced ammonia-sensing properties of PANI-TiO2-Au ternary self-assembly nanocomposite thin film at room temperature, Sens. Actuators B 246 (2017) 85–95.

[16] Keqing Zhanga, Xinli Jinga, Preparation and characterization of polyaniline with high electrical conductivity, Polym. Adv. Technol. 20 (2009) 689–695.

[17] V. Dixit, S.C.K. Misra, B.S. Sharma, Carbon monoxide sensitivity of vacuum deposited polyaniline semiconducting thin films, Sens. Actuators B 104 (2005) 90–93.

[18] Pavol Kunzo, Peter Lobotka, Matej Micusik, Eva Kovacova, Palladium-free hydrogen sensor based on oxygen-plasma-treated polyaniline thin film, Sens. Actuators B 171–172 (2012) 838–845.

[19] Zhubo Liu, A.V. Rogachev, Bing Zhou, M.A. Yarmolenko, A.A. Rogachev, D.L. Gorbachev, Xiaohong Jiang, Effects of polyvinyl chloride and aluminum trichloride on structure and property of polyaniline composite films by electron beam deposition, Polym. Eng. Sci. 53 (2013) 502–506.

[20] A.A. Ragachev, M.A. Yarmolenko, Jiang Xiaohong, Ruiqi Shen, P.A. Luchnikov, A.V. Rogachev, Molecular structure, optical, electrical and sensing properties of PANI-based coatings with silver nanoparticles deposited from the active gas phase, Appl. Surf. Sci. 351 (2015) 811–818.

[21] J. Evgenij Barsoukov (Ed.), Impedance Spectroscopy Theory, Experiment, and Applications, Ross Macdonald Wiley & Sons, Inc., 2005, p. 606.

[22] Zuzana Rozlívková, Miroslava Trchová, Ivana Šeděnková, Milena Špírková, Jaroslav Stejskal, Structure and stability of thin polyaniline films deposited in situ on silicon and gold during precipitation and dispersion polymerization of aniline hydrochloride, Thin Solid Films 519 (2011) 5933–5941.

[23] Ivana Sedenkova, Miroslava Trchova, Jaroslav Stejskal, Thermal degradation of polyaniline films prepared in solutions of strong and weak acids and in

water – FTIR and Raman spectroscopic studies, Polym. Degrad. Stab. 93 (2008) 2147–2157.
[24] M.C. Bernard, A. Hugot-Le Goff, Quantitative characterization of polyaniline films using Raman spectroscopy I: polaron lattice and bipolaron, Electrochim. Acta 52 (2006) 595–603.
[25] Miroslava Trchová, Zuzana Morávková, Michal Bláha, Jaroslav Stejskal, Raman spectroscopy of polyaniline and oligoaniline thin films, Electrochim. Acta 122 (2014) 28–38.
[26] Liming Wang, Qin Yao, Hui Bi, Fuqiang Huang, Qun Wang, Lidong Chen, Large thermoelectric power factor in polyaniline/graphene nanocomposite films prepared by solution-assistant dispersing method, J. Mater. Chem. A 2 (2014) 11107–11113.
[27] Vanish Kumar, Rashmi Mahajan, Deepika Bhatnagar, Inderpreet Kaur, Nanofibers synthesis of ND:PANI composite by liquid/liquid interfacial polymerization and study on the effect of NDs on growth mechanism of nanofibers, Eur. Polym. J. 83 (2016) 1–9.
[28] Miroslava Trchová, Zuzana Morávková, Ivana Šeděnková, Jaroslav Stejskal, Spectroscopy of thin polyaniline films deposited during chemical oxidation of aniline, Chem. Pap. 66 (2012) 415–445.
[29] Anjali A. Athawale, Milind V. Kulkarni, Vasant V. Chabukswar, Studies on chemically synthesized soluble acrylic acid doped polyaniline, Mater. Chem. Phys. 73 (2002) 106–110.
[30] J.E. Albuquerque, L.H.C. Mattoso, D.T. Balogh, R.M. Faria, J.G. Masters, A.G. MacDiarmid, A simple method to estimate the oxidation state of polyanilines, Synth. Met. 113 (2000) 19–22.
[31] Jaroslav Stejskal, Miroslava Trchova, Aniline oligomers versus polyaniline, Polym. Int. 61 (2012) 240–251.
[32] S. Banerjee, S. Sarmah, A. Kumar, Photoluminescence studies in HCl-doped polyaniline nanofibers, J. Opt. 38 (2009) 124–130.
[33] Wolfgang Haiss, Nguyen T.K. Thanh, Jenny Aveyard, David G. Fernig, Determination of size and concentration of gold nanoparticles from UV–vis spectra, Anal. Chem. 79 (2007) 4215–4221.
[34] Yiqin Chen, Xuezeng Tian, Wei Zeng, Xupeng Zhu, Hailong Hu, Huigao Duan, Vapor-phase preparation of gold nanocrystals by chloroauric acid pyrolysis, J. Colloid Interface Sci. 439 (2015) 21–27.
[35] Steven D. Perrault, Warren C.W. Chan, Synthesis and surface modification of highly monodispersed, spherical gold nanoparticles of 50–200 nm, J. Am. Chem. Soc. 131 (131) (2009) 17042–17043.
[36] Moon Gyu Han, Seung Soon Im, X-ray photoelectron spectroscopy study of electrically conducting polyaniline/polyimide blends, Polymer 41 (2000) 3253–3262.
[37] Sebastian Golczak, Anna Kanciurzewska, Mats Fahlman, Krzysztof Langer, Jerzy J. Langer, Comparative XPS surface study of polyaniline thin films, Solid State Ionics 179 (2008) 2234–2239.
[38] Jana Tabaciarova, Matej Micusík, Pavol Fedorko, Maria Omastova, Study of polypyrrole aging by XPS, FTIR and conductivity measurements, Polym. Degrad. Stab. 120 (2015) 392–401.
[39] R.F. Bianchi, H.N. da Cunha, R.M. Faria, G.F. Leal Ferreira, J. Mariz, G. Neto, Electrical studies on the doping dependence and electrode effect of metal-PANI-metal structures, J. Phys. D: Appl. Phys. 38 (2005) 1437–1443.